Available online: 26 May 2020
DOI: 10.1021/acs.inorgchem.0c00953
Cite this: Inorg. Chem. 2020, 59, 12, 8543–8551

Electronic structure of the vanadium intercalated and substitutionally doped transition metal dichalcogenides $Ti_xV_ySe_2$

Alexey S. Shkvarin[1,*], Yury M. Yarmoshenko[1], Alexander I. Merentsov[1], Elena G. Shkvarina[1], Andrei F. Gubkin[1], Igor Píš[2,3], Silvia Nappini[3], Federica Bondino[3], Ivan A. Bobrikov[4], Alexander N. Titov[1]

[1]M.N. Miheev Institute of Metal Physics of Ural Branch of Russian Academy of Sciences, 620990 Ekaterinburg, Russia

[2]Elettra-Sincrotrone Trieste S.C.p.A, S.S. 14 – km 163.5, 34149 Basovizza, Trieste, Italy

[3]IOM-CNR, Laboratorio TASC, S.S. 14 – km 163.5, 34149 Basovizza, Trieste, Italy

[4]Joint Institute for Nuclear Research, ul. Joliot-Curie 6, 141980 Dubna, Moscow oblast, Russia

*shkvarin@imp.uran.ru

Abstract

Electronic structure of the $TiSe_2$ dichalcogenide intercalated with V and substitutionally doped $Ti_{1-x}V_xSe_2$ have been studied using soft X-ray photoelectron, resonant photoelectron and absorption spectroscopy. In the case of the substitution of Ti by V the formation of the coherently oriented structural fragments VSe_2 and $TiSe_2$ is observed and a small charge transfer between these fragments is found. The intercalation of the V atoms into the $TiSe_2$ leads to the charge transfer from the V atoms to the Ti with the formation of covalent complexes Ti-Se_3-V-Se_3-Ti.

Introduction

Quasi-two-dimensional materials based on titanium dichalcogenides have attracted attention in the last decades. These materials demonstrate superconductivity[1], a state with a charge density wave[2], spin polarization[3]. The crystal structure of these materials consists of Ch-Ti-Ch layers, where Ch is S, Se, Te. These Ch-Ti-Ch layers are usually called a “sandwich”. The interaction between the atoms within the "sandwich" is strong, whereas the chemical bond between "sandwiches" is weak (it is historically called van der Waals bond). The interlayer gap between the "sandwiches" is also called the van der Waals gap. This weak chemical bond between sandwiches allows the intercalation of various atoms or molecules into the van der Waals gap[4]. It can significantly modify the electronic structure of the host material.

Another way to change the electronic structure, without a critical change in the crystal structure, is the substitution of the titanium atom directly in the host lattice

by another atom with an ionic radius of similar size. The substitution of Ti by V is a good choice in the case of $TiSe_2$. The physical properties[5] and the crystal structure[6] of $TiSe_2$, intercalated with vanadium, have been studied previously. The compounds with the substitution of the Ti by V are more widely studied: physical properties[7,8], crystal[7,9] and electronic structure[9] of these compounds have already been studied. The starting materials $TiSe_2$ and VSe_2 have been studied for a long time[10,11,20,12–19]. A comparative analysis of the electronic structure of the compositions with substitution and intercalation has not been performed yet.

The vanadium atom has an electronic configuration of $3d^34s^2$, whereas the configuration of the titanium atom is $3d^24s^2$. So, V has an extra electron after four electrons are used to fill the 4p level of two Se atoms. This electron will be either localized around the doping V atom or delocalized in the Ti 3d band depending on the relative energies of the different states.

The available data for the intercalation compounds are deficient. The vanadium atoms occupy the octahedral positions of the interlayer space [6]. Therefore, the V atoms are coordinated by the chalcogen, similarly to the titanium atoms, which can be substituted by the vanadium. The fundamental difference is in the composition of the second coordination sphere. For intercalated vanadium atom, the neighbors in the second coordination sphere along the *c*-axis are titanium atoms, while in case of substitution the second coordination sphere of V along the *c*-axis contains vacant positions (due to the van der Waals gap). Therefore, the hybridization of the V $3d_{zz}$ with Ti $3d_{zz}$ states can be expected in case of intercalated vanadium. In case of substitution atomic-like nature can be expected because contact Ti_{xy} and Ti_{xx-yy} orbitals are empty.

We propose two modifications of the crystal structure at the vanadium introduction, which model structures are shown in Fig.1. The model crystal structures in the case of intercalation and substitution of vanadium are shown in Fig. 1, left and right panels, correspondingly.

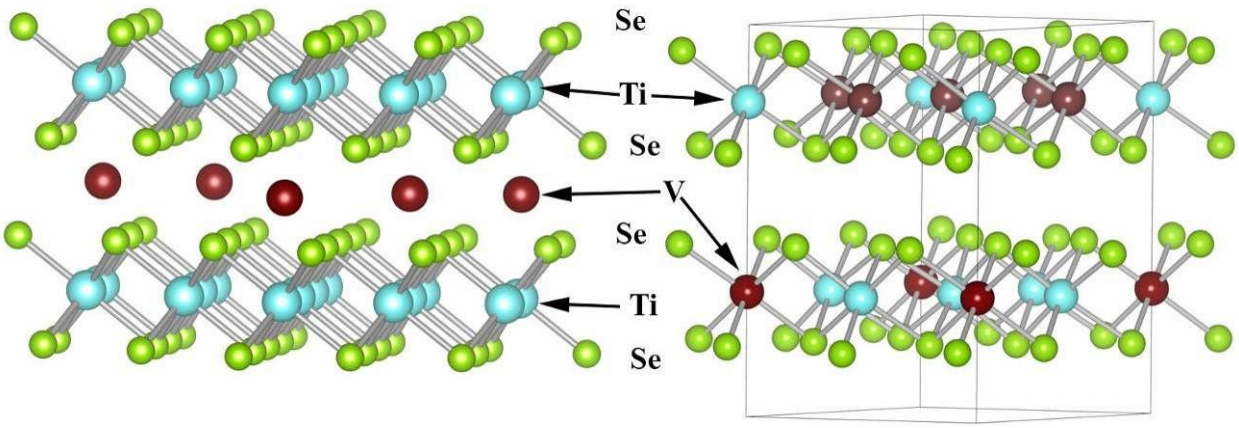

Figure 1. The model crystal structure for the intercalated (left) and substitution (right) compounds.

In this work we studied different influence of $TiSe_2$ doping with vanadium on the electronic structure of $TiSe_2$ depending on the type of doping. The intercalation of vanadium (V_xTiSe_2) was performed for the first time. The substitution of Ti by V ($Ti_{1-x}V_xSe_2$) was performed previously[9], in these work we compare those data with new ones obtained with better quality. The electronic structure of these materials was studied using the X-ray photoelectron spectroscopy (XPS), resonant photoelectron spectroscopy (ResPES) and X-ray absorption spectroscopy (XAS).

Experiment

Single crystal samples were grown in sealed quartz ampoules using the gas-transport reaction technique[21]. The titanium (after iodine purification, 99.95%), vanadium (99.95%) and selenium (OSCh19-5, 99.999%) were used as starting materials. Synthesis was carried out in sealed quartz ampoules evacuated to 10^{-5} torr. The synthesis procedure was described in more detail elswhere[22]. We managed to grow single crystals with the following compositions: i) $Ti_{0.9}V_{0.1}Se_2$, $Ti_{0.28}V_{0.83}Se_2$, $Ti_{0.17}V_{0.9}Se_2$ (substitionally doped) and ii) $V_{0.04}TiSe_2$, $V_{0.08}TiSe_2$ (intercalation compounds).

The single crystals of $V_xTi_{1-x}Se_2$ were grown using gas-transport reaction technique in evacuated sealed quartz ampoules of 12 - 15 cm length with iodine as a carrier gas. The ampoule was placed into the furnace with nearly linear temperature gradient with the temperatures of 1000 ^oC on the hot end and 400 ^oC on the cold end. The charge of the homogenized material was at a temperature of ~ 900 ^oC, and the mass transfer was from the hot end to the cold end. The $V_xTi_{1-x}Se_2$ single crystals were grown at temperatures of 600 - 700 ^oC and the chemical composition of the crystals always corresponded to that of the charge.

The structure and phase purity of the powder $Ti_xV_ySe_2$ samples were studied using X-ray powder diffraction technique (XRD) in the Institute of Metallurgy UrD RAS, CUC "Ural-M" using diffractometer Shimadzu XRD 7000 Maxima (Cu Kα radiation, graphite monochromator). The models of the crystal structure of the $V_xTi_{1-x}Se_2$ [9] and V_xTiSe_2 [6] has been published earlier.

The intercalated V_xTiSe_2 single crystals were grown at the same conditions, but the crystals were formed at the hot side of the ampoule at the temperatures of 900 - 950 ^oC. At the same time, the crystals of $V_xTi_{1-x}Se_2$ with different Ti and V concentrations were formed on the cold end of this ampoule. The chaotic variation in composition makes these crystals inappropriate for the further systematic

investigation. The chemical composition of the V_xTiSe_2 crystals was limited by the low concentrations of the intercalated vanadium. It should be noted that we didn't observe the formation of the $TiSe_2$ crystals on the hot end of the ampoule during the growth of the intercalated V_xTiSe_2 crystals.

The chemical composition was determined using X-ray fluorescence analysis on a JEOL-733 spectrometer. It should be noted that the stoichiometry of the metal atoms in V-substituted $TiSe_2$ exceeds 1, i.e. (Ti + V): Se > 1:2. This means that in these materials slight intercalation of metal atoms in addition to the dominant substitution of Ti by V can occur.

More successful growth of the $Ti_{1-x}V_xSe_2$ single crystals in comparison with V_xTiSe_2 single crystals indicates that the position of vanadium in the regular lattice is more stable than in the interlayer space. This means that in substitution compounds with an excess of metal ((Ti + V): Se > 1:2) most likely titanium is in excess and occupies the positions in the interlayer space.

In order to prove this model of crystal structure, we performed a neutron diffraction study of the $V_{0.6}Ti_{0.6}Se_2$ powder sample using high-resolution Fourier diffractometer (HRFD) [23] at the IBR-2 pulsed reactor in Dubna, Russia. The neutron diffraction patterns were analyzed by the Rietveld method with the aid of the FullProf software package [24]. A model of the trigonal crystal structure described with the space group *P*-3*m*1 (№164) [25] has been used to fit the neutron diffraction patterns. Visualization of the best fit result for $V_{0.6}Ti_{0.6}Se_2$ is shown in the Supplementary. The refined values of the unit cell parameters and atomic coordinates are shown in table 1. As one can see from table 1, a slightly non-random cation distribution between layers in the sandwich-like structure was proved by the neutron diffraction. Ti ions preferentially occupy 1*b* Wyckoff site between the Ch-*M*-Ch layers while V ions preferentially occupy 1*a* Wyckoff site inside of Ch-*M*-Ch layers. The similar behavior was previously reported for $Fe_{7-y}M_yX_8$ chalcogenides (X = S, Se; M = Ti, Co) [26].

Таблица 1. Atomic coordinates, site occupancies, unit cell parameters and corrected for background agreement factors obtained for $V_{0.6}Ti_{0.6}Se_2$.

Atom	$x(\delta x)$	$y(\delta y)$	$z(\delta z)$	Occupancy
Ti(1a)	0	0	0	0.45(1)
V(1a)	0	0	0	0.54(1)

Ti(1b)	0	0	1/2	0.13(1)
V(1b)	0	0	1/2	0.06(1)
Se(2d)	1/3	2/3	0.2585(2)	1
Unit cell:	a=3.52686(3) Å, c=5.98026(5) Å			
Agreement factors:	$\chi^2 = 2.3$, $R_B = 12.9\%$, $R_{wp}=9.1\%$, $R_{exp}=6.2\%$			
	Refined stoichiometry: $V_{0.60(2)}Ti_{0.58(2)}Se_2$			

The XPS, XAS and ResPES spectra of $Ti_xV_ySe_2$ were obtained at room temperature (RT) on the BACH beamline [27]of the Elettra synchrotron facility (Trieste, Italy). All of the samples were cleaved at RT in a vacuum chamber in a pressure better than 1×10^{-9} Torr. The purity of the surface was confirmed by the absence of oxygen and carbon peaks in the survey spectra. The photon energy resolution was set to 0.1 eV at Ti L-edge and 0.15 eV at V L-edge, respectively. Ti and V $L_{2,3}$ XAS were performed in total electron yield mode and calibrated using the corresponding absorption spectra of the pure metals. Photoemission spectra were measured with a Scienta R3000 electron energy analyzer at normal emission with an energy resolution better than 0.25 eV. Binding energies were calibrated to the Au $4f_{7/2}$ signal from a clean gold foil (E_B ($4f_{7/2}$) = 84.0 eV). All the core-level XPS spectra were measured at a photon energy of 602 eV.

Multiplet calculations of the V absorption spectra were performed using the program ctm4XAS [28]. The calculation parameters are listed in Table 2. The Slater parameter determines the change in Slater integrals contribution that corresponds for the compounds under discussion to the change in the ratio of covalent and ionic components in a chemical bond. The10Dq parameter determines the splitting in the crystal field. The SO parameter determines the spin-orbit splitting. The Δ parameter is the charge transfer energy or the energy between $3d^n$ and $3d^{n+1}$ states. The U_{pd} parameter determines the value of the hole potential (describes the interaction between d electron and core 2p hole). The e_g and t_{2g} parameters determine the hybridization of corresponding orbitals. It should be noted that the parameters resulting from the calculation are only adjustable parameters; therefore, we can estimate only the change of the physical properties rather than the exact quantitative values.

Table 2. Multiplet Calculation Parameters for V^{+4}

Sample	Slater, %	10Dq, eV	Δ, eV	U_{dd}-U_{pd}, eV	S-O, %	e_g, eV	t_{2g}, eV
VSe_2	50	1.15	3	4.5	104	2.4	1.1

Result and discussion

XPS

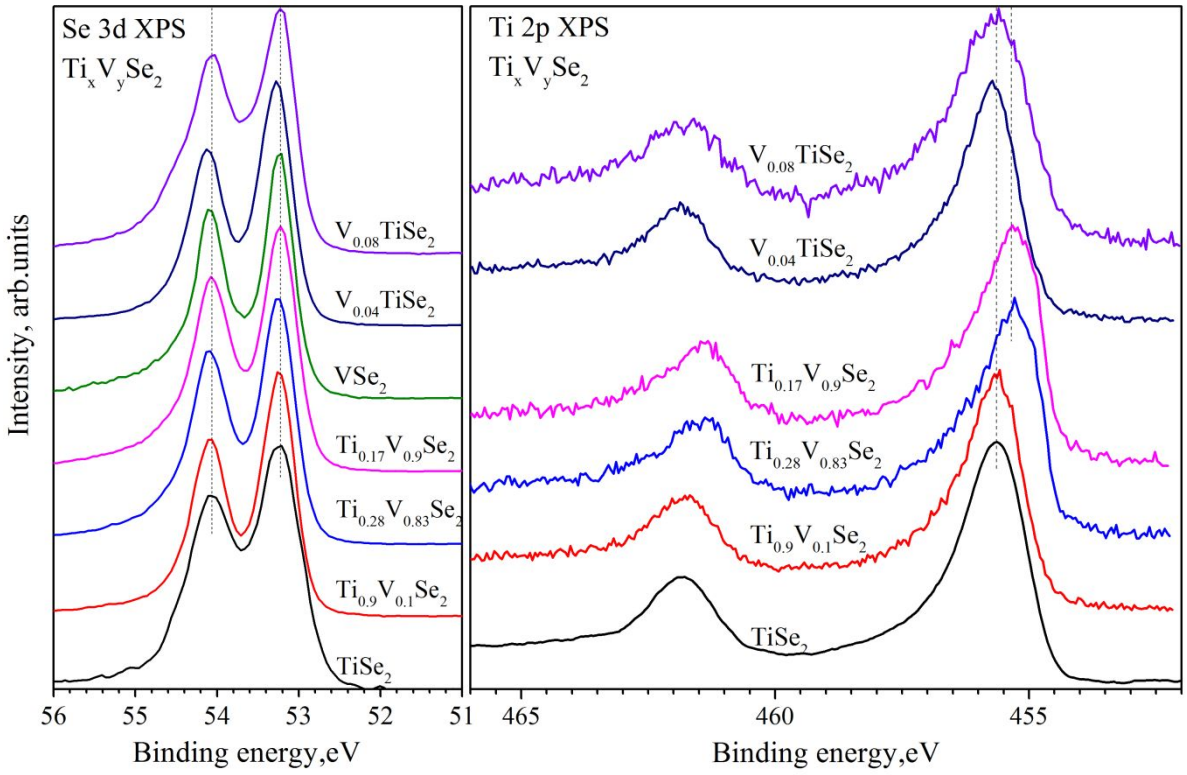

Figure 2. Left panel: XPS Se 3d core level for $Ti_xV_ySe_2$. Right panel: XPS Ti 2p core level for $V_yTi_xSe_2$.

The Se 3d core level spectra are shown in Fig. 2 (left panel). Most of the spectra have the same shape and energy position and are in agreement with our previous results[9]. The only spectrum which shape differs from the others is one for $V_{0.08}TiSe_2$. It appears to have a shoulder on the higher binding energy side. This is caused by the presence of two nonequivalent crystallographic positions of selenium with different local environment [29,30].

The Ti 2p core level spectra are shown in Fig. 2 (right panel). The shape of all the spectra is nearly the same. At high concentration of substitutional vanadium, an energy shift of 0.2 eV of the spectra toward the low binding energies is observed, which also coincides with previous results[9]. At the same time, the spectra for the

materials with intercalated vanadium are slightly shifted toward high binding energies.

For the $V_{0.08}TiSe_2$ compound a considerable broadening of the Ti 2p spectrum is observed. We have already observed a similar broadening for Mn_xTiSe_2 [31] and Fe_xTiSe_2 [32] systems with respect to $TiSe_2$ previously. The reason for this broadening is the formation of two unequivalent crystallographic positions of titanium atoms: with or without vanadium atom in the second coordination sphere.

XAS

The Ti $L_{2,3}$ XAS spectra are shown in Fig. 3 (left panel).

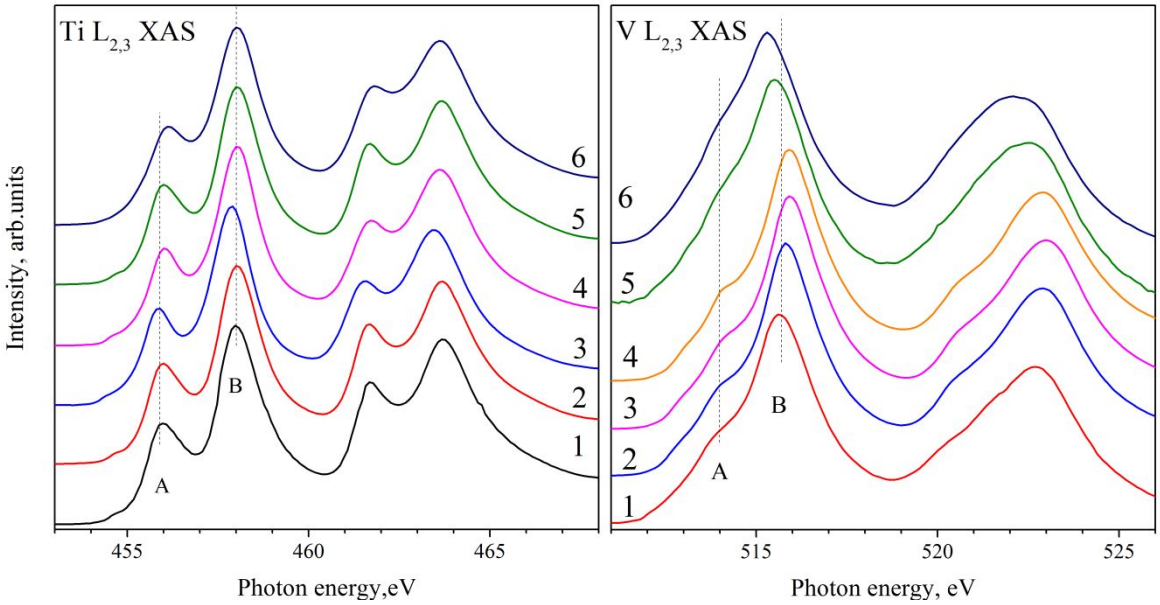

Figure 3. Left panel: Ti $L_{2,3}$ XAS for $Ti_xV_ySe_2$ (1. $TiSe_2$; 2. $Ti_{0.9}V_{0.1}Se_2$; 3. $Ti_{0.28}V_{0.83}Se_2$; 4. $Ti_{0.17}V_{0.9}Se_2$; 5. $V_{0.04}TiSe_2$; 6. $V_{0.08}TiSe_2$;). Right panel: V $L_{2,3}$ XAS for $Ti_xV_ySe_2$ (1. $Ti_{0.9}V_{0.1}Se_2$; 2. $Ti_{0.28}V_{0.83}Se_2$; 3. $Ti_{0.17}V_{0.9}Se_2$;4. VSe_2; 5. $V_{0.04}TiSe_2$; 6. $V_{0.08}TiSe_2$;).

A change in the energy position for A and B peaks is observed only for the compound with the highest content of the intercalated vanadium (x = 0.08). The distance between these peaks for this compound is the lowest as compared to other compounds. This behaviour indicates[33] the increase in the covalent contribution to the chemical bond between titanium and the nearest environment and, consequently, the formation of the Ti-V-Ti covalent centres.

The V $L_{2,3}$ XAS spectra are shown in Fig. 3 (right panel). The energy position of the spectra and their shape is almost the same for all the compounds with vanadium substitution and are similar to the spectrum for VSe_2. The increase in the vanadium content leads to a slight shift (~ 0.1 eV) of the spectra toward the high photon energies. The intensity of the A peak also slightly increases with vanadium

content. The vanadium intercalation in V_xTiSe_2 leads, vice versa, to a shift of V $L_{2,3}$ toward the low photon energies. The energy shift is of 0.28 eV for $V_{0.04}TiSe_2$ and of 0.52 eV for $V_{0.08}TiSe_2$.

The result of the V $L_{2,3}$ multiplet calculation for VSe_2 is shown in fig. 4.

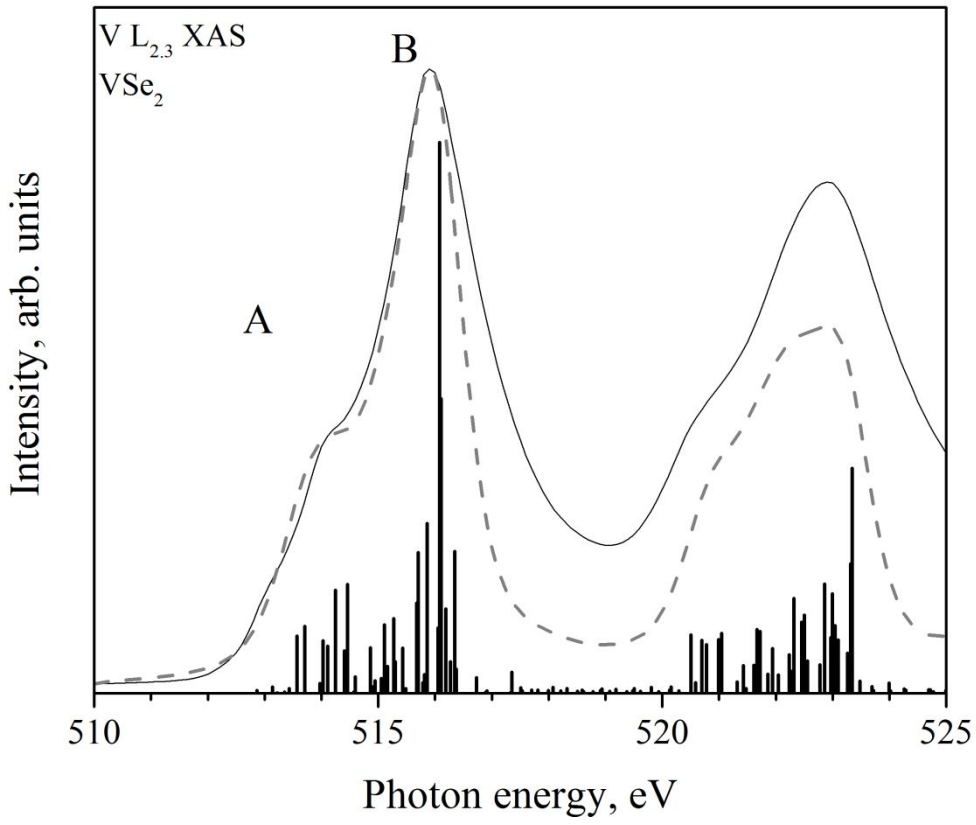

Figure 4. V $L_{2,3}$ XAS multiplet calculation for VSe_2 (V^{4+}). Solid line - experimental spectrum, dashed line - calculation.

The A-B peak separation in V $L_{2,3}$ XAS is mainly determined by the value of the multiplet splitting 10Dq, as it is for the same peak in Ti $L_{2,3}$ XAS. In a similar way to Ti $L_{2,3}$ spectra, we can assume that the decrease of the A-B peak distance in V $L_{2,3}$ XAS is due to the increase of the covalent contribution to the chemical bond between vanadium atom and the nearest environment.

Valence band spectra

Fig. 5 shows the valence band (VB) spectra for the $Ti_xV_ySe_2$ samples. All of the spectra have similar shape. The main maximum in the binding energy range of 0 - 6 eV contains M, N, Q and T peaks and is due to the hybridization of the metal 3d and Se 4p states. Se peak in the range of 12-14 eV is a Se 4s peak. These 5 peaks are the same as for the undoped $TiSe_2$ [33]. The main difference in the spectra is in the intensity of the R peak, which energy is directly below the Fermi level. The intensity of resonant peak for the substitutional compounds with high V content is higher than that in ref.[9] due to the better resolution of the VB spectrum. For VSe_2

this peak can be only due to V 3d states, but for another compounds the Ti 3d states may also give a contribution into this peak.

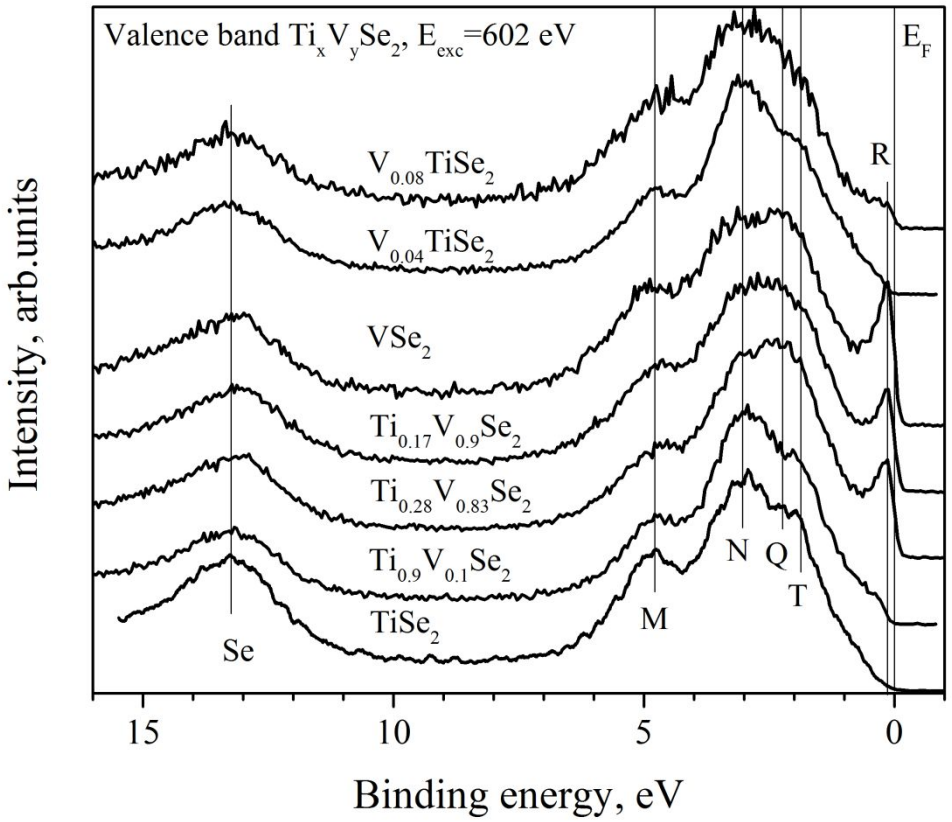

Figure 5. VB spectra for $Ti_xV_ySe_2$

To separate the contributions from Ti and V into the R peak the resonant photoelectron spectra were obtained.

ResPES

Element-specific information about the energy localization of the electronic states can be obtained by resonant photoelectron spectroscopy [34–38].

The VB spectra for $Ti_{0.9}V_{0.1}Se_2$ obtained in the Ti 2p-3d resonant excitation mode are shown in fig. 6, upper panel, as an example. From left to right are shown: experimental VB spectra obtained at different excitation energies, difference spectra after processing [39], Ti $L_{2,3}$ XAS with excitation energy scale (it corresponds to the photon energy for XAS). The coloured area in the central part of the upper panel clearly shows the intensity of the difference valence band spectra. Lower panel of the Fig. 6 shows Ti 2p-3d ResPES spectra for all of the studied samples after additional processing [39] overlaid with the corresponding Ti $L_{2,3}$ XAS.

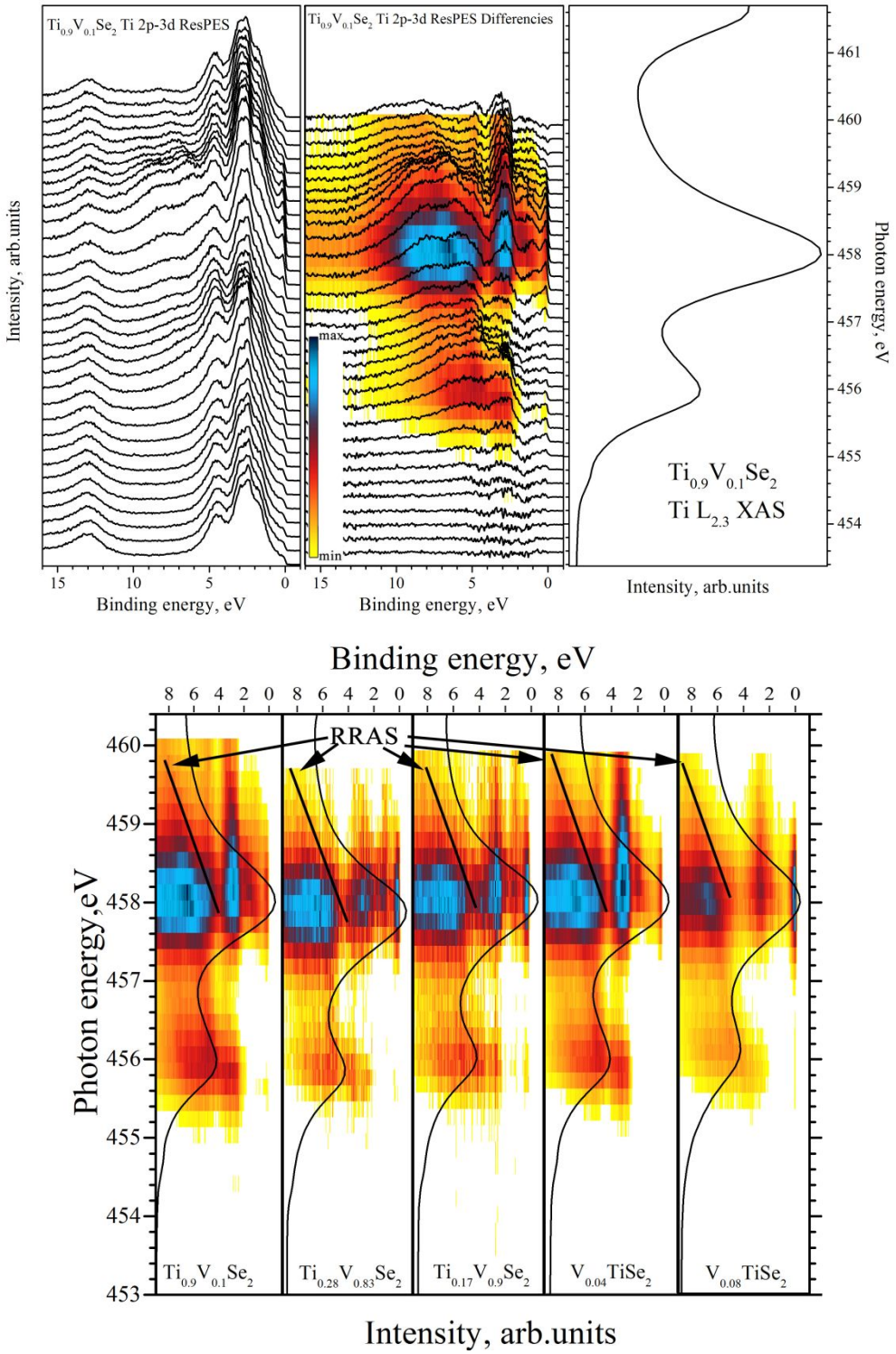

Figure 6. Upper panel: Ti 2p – 3d ResPES for $Ti_{0.9}V_{0.1}Se_2$. The difference spectra, which were obtained by the method described in Ref. [39], are shown in the central part of the panel in the form of an image plot. Lower panel: VB spectra obtained in Ti 2p-3d resonant excitation mode after additional processing. The VB spectra are overlaid with corresponding Ti $L_{2,3}$ XAS.

Ti 2p-3d ResPES spectra for the compounds with vanadium substitution have the similar structure. Two main regions are visible for the compounds with low ($x<0.5$) vanadium content. There are two regions for the samples with low vanadium concentrations, where the resonant peak is visible. These regions

coincide with the peaks on the Ti $L_{2,3}$ XAS (A and B peaks in Fig. 3). The intensity of the R resonant peak is less than that of RRAS (resonant Raman Auger scattering). For the $V_xTi_{1-x}Se_2$ samples with high vanadium concentrations ($x \geq 0.5$) the intensity of the R peak comes up to that of RRAS and is further independent on the vanadium content (see Fig. 7). It should be noted that the overall intensity of the spectra (Fig. 6) decreases due to the decrease of the vanadium concentration. For the intercalation compounds V_xTiSe_2 one can see from Fig.6 that the resonant peak corresponds in the excitation energy to the main maximum of the absorption spectrum (peak B in Fig. 4). The intensity of the resonant peak increases significantly with increase in the vanadium concentration (see Fig. 7, upper spectra).

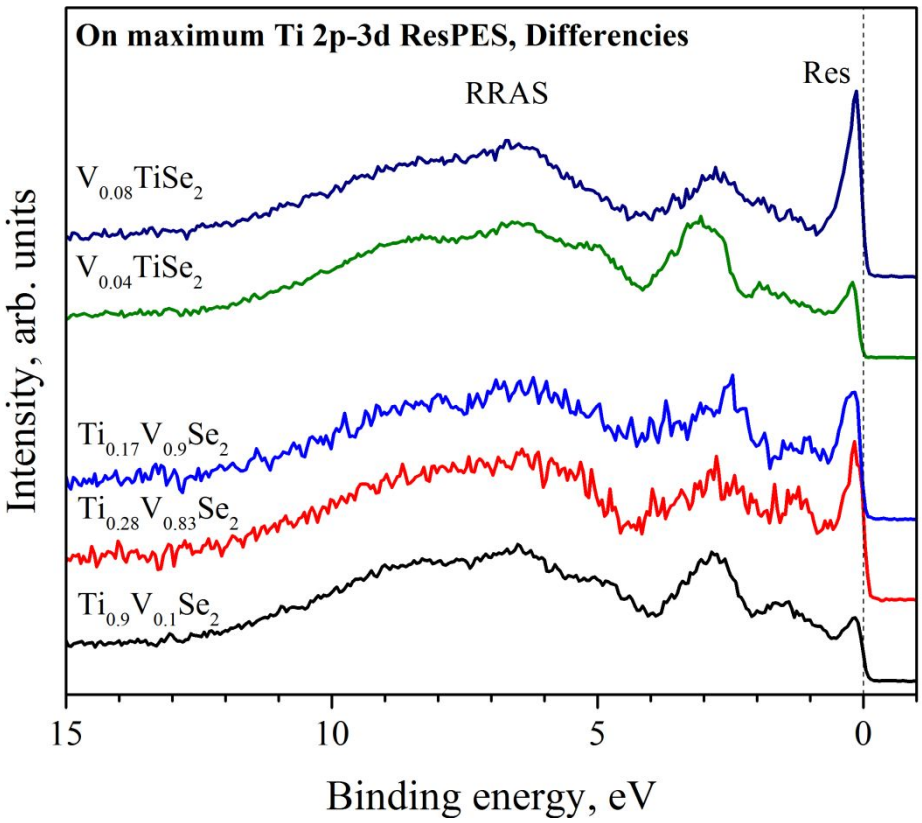

Figure 7. Ti 2p-3d ResPES on maximum difference spectra. The ratio I_{res}/I_{RRAS} equals to: 0.47 for $Ti_{0.9}V_{0.1}Se_2$; 1.15 for $Ti_{0.28}V_{0.83}Se_2$; 0.96 for $Ti_{0.17}V_{0.9}Se_2$; 0.55 for $V_{0.04}TiSe_2$; 1.41 for $V_{0.08}TiSe_2$.

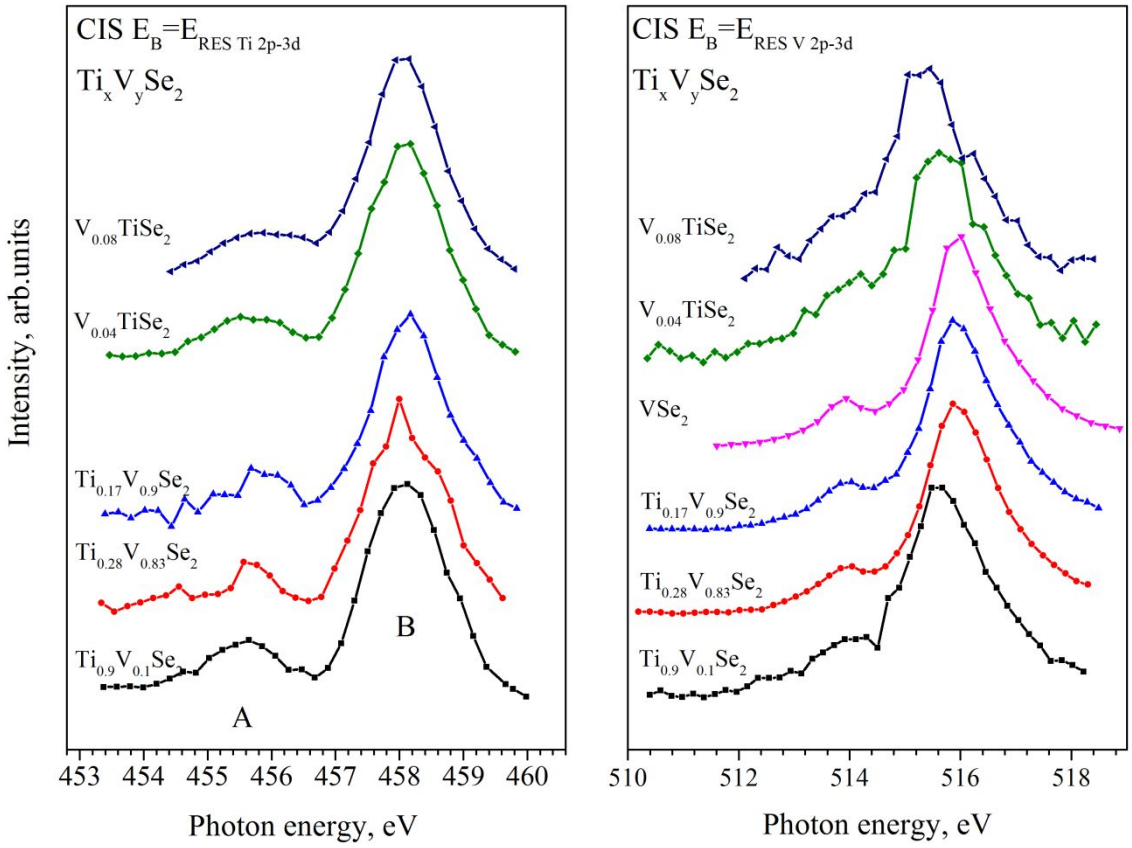

Figure 8. CIS spectra at 0.15 eV binding energy, obtained from Ti 2p - 3d (left panel) and V 2p-3d (right panel) ResPES.

Fig.8 (left panel) shows CIS (constant initial states) spectra obtained directly from the Ti 2p-3d ResPES spectra. The I_A/I_B ratios obtained from CIS are listed in Table 3, while the energy position of A and B peaks is seen from fig. 3.

Table 3. I_A/I_B for $Ti_xV_ySe_2$ CIS for Ti 2p-3d ResPES spectra in Fig. 8 (left)

Sample	$Ti_{0.9}V_{0.1}Se_2$	$Ti_{0.28}V_{0.83}Se_2$	$Ti_{0.17}V_{0.9}Se_2$	$V_{0.04}TiSe_2$	$V_{0.08}TiSe_2$
I_A/I_B	0.25(1)	0.25(1)	0.23(1)	0.19(1)	0.19(1)

The increase in vanadium concentration in case of substitution leads to a decrease of I_A/I_B ratio in CIS spectra. In case of substitution this decrease is low, while in case of intercalation it changes 1.3 times as compared to that for $Ti_{0.9}V_{0.1}Se_2$

The conclusion about the spatial distribution of the electrons from titanium can be drawn based on Ti 2p-3d ResPES. Because the A peak in Fig 3 is caused by Ti t_g (d_{xy}, d_{xz} and d_{yz}) states and B peak by Ti e_g (d_z^2 and d_x^2-$_y^2$) states [40], the electrons on the Ti atoms are distributed between e_g and t_{2g} states. It must be noted, that we use scheme of orbital distribution which is proposed for titanium dichalcogenides in [41]. According to this scheme, we re-designate the d-orbitals of both transition metals

in the layer and intercalated metals in accordance with the crystallographic axes. As one can see from Table 3, the relative contribution of the e_g states compared with t_{2g} states is higher for the intercalated V_xTiSe_2 compounds than for the substitutional ones. Consequently, the Ti $3d_z^2$ (corresponds to the direction toward vanadium atoms in the interlayer space) and $3d_{x^2-y^2}$ orbitals (correspond to the direction toward other titanium atoms in the lattice) are mainly filled. Since there is no resonant peak in the pristine $TiSe_2$ [42], this peak is due to the hybridization of the Ti $3d_z^2$ orbitals with V $3d_z^2$ orbitals.

Fig. 9 shows V 2p-3d ResPES spectra. All the spectra were additionally processed [39].

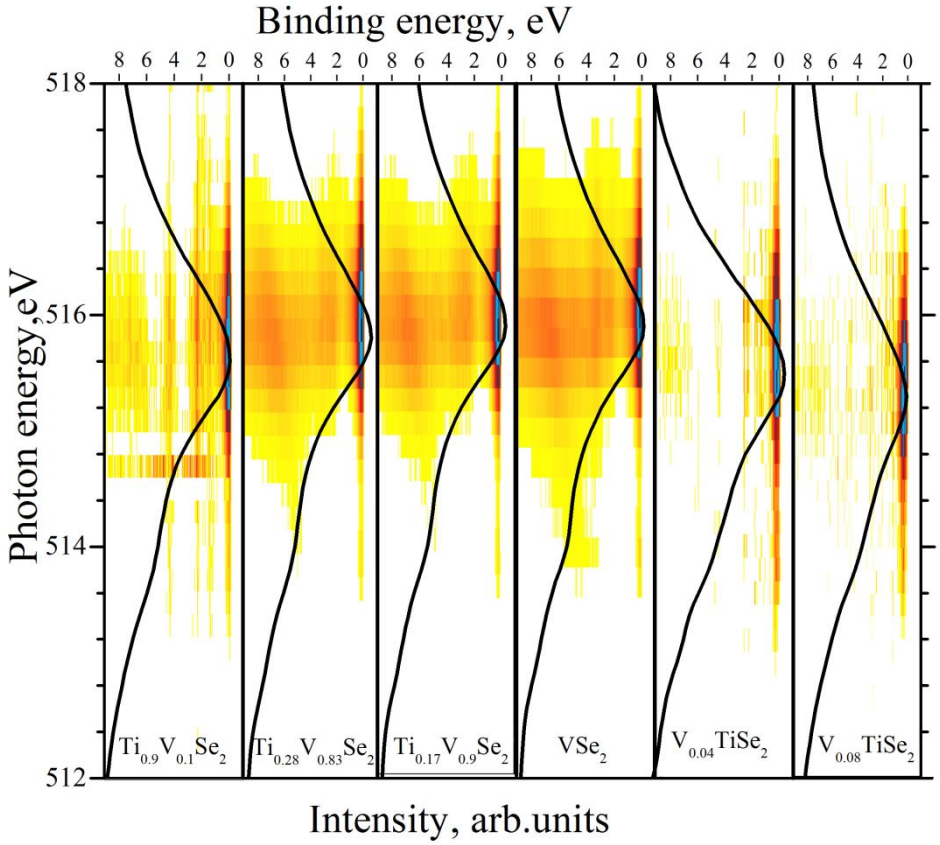

Figure 9. V 2p-3d ResPES after additional processing. The VB spectra are overlaid with corresponding V $L_{2,3}$ XAS

Table 4. I_A/I_B for $Ti_xV_ySe_2$ V 2p-3d ResPES CIS

Sample	$Ti_{0.9}V_{0.1}Se_2$	$Ti_{0.28}V_{0.83}Se_2$	$Ti_{0.17}V_{0.9}Se_2$	VSe_2	$V_{0.04}TiSe_2$	$V_{0.08}TiSe_2$
I_A/I_B	0.19(2)	0.19(2)	0.19(2)	0.19(2)	0.11(2)	0.09(2)

For the $V_xTi_{1-x}Se_2$ compounds the spectra obtained in the V 2p-3d resonant excitation mode look nearly the same (taking into account the vanadium concentration) and are similar to the spectra of pristine VSe_2. Two resonant regions

can be distinguished. The first one corresponds to the excitation energy range of peak A, the second one - to the excitation energy range of peak B of the absorption spectra V $L_{2,3}$ (Fig. 3). This allows suggesting that the VSe_2 structural fragments remain in this material, rather than vanadium randomly substitute the titanium atoms.

For the V_xTiSe_2 compounds a sharp decrease in the intensity of the RRAS contribution is observed as compared to the resonant peak. Only resonant peak at binding energy around 0.15 eV is observed as compared to $V_xTi_{1-x}Se_2$. From Fig. 8, right panel, it can be seen that in the compositions with substitution a peak at a photon energy of about 514 eV is well observed. In the intercalated compounds, this peak is practically not visible.

Since e_g states have a higher energy than t_{2g} states also for vanadium [43], the B peak in the absorption spectra can be associated to e_g states, and the A peak - to the t_{2g} states. In this case, as for the titanium resonance, it can be seen that for $V_xTi_{1-x}Se_2$ the vanadium electrons are distributed over all of the orbitals, whereas for V_xTiSe_2 they are distributed mainly over the e_g orbitals, which have a direction toward the titanium atoms.

Conclusions

The $Ti_xV_ySe_2$ electronic structure in the case of intercalation of the V atoms and in the case of the substitution of Ti by V atoms has been studied experimentally. It was confirmed that a weak interaction between $TiSe_2$ and VSe_2 structural fragments occurs in the case of the substitution even at high vanadium concentration, as it has been proposed in our previous work[9]. In the case of intercalation the charge transfer between the Ti and V atoms is observed experimentally. The valence band spectra at the Ti 2p-3d and V2p-3d resonant excitation mode show the spatial distribution of the 3d electrons of Ti and V.

Acknowledgments

The research was carried out within the state assignment of the Ministry of Education and Science of Russia (theme “Electron” No. AAAA-A18-118020190098-5, theme “Flux” No. AAAA-A18-118020190112-8 and theme “Spin” No. AAAA-A18-118020290104-2) and with partial financial support of the RFBR (project 19-33-60031). Authors are grateful for synchrotron ELETTRA for support of experimental Project Nos. 20160215 and 20160193; the results obtained were used in this work.

References

(1) Morosan, E.; Zandbergen, H. W.; Dennis, B. S.; Bos, J. W. G.; Onose, Y.; Klimczuk, T.; Ramirez, A. P.; Ong, N. P.; Cava, R. J. Superconductivity in CuxTiSe2. *Nat. Phys.* **2006**, *2* (8), 544–550.

(2) Rossnagel, K. On the Origin of Charge-Density Waves in Select Layered Transition-Metal Dichalcogenides. *J. Phys. Condens. Matter* **2011**, *23* (21), 213001.

(3) Shkvarin, A. S.; Yarmoshenko, Y. M.; Skorikov, N. A.; Merentsov, A. I.; Titov, A. N.; Slepukhin, P. A.; Marchenko, D. E.; Sperling, M. Studying the Electronic Structure of Cr x Ti1-x Se2 by X-Ray Resonance and Absorption Spectroscopy. *J. Exp. Theor. Phys.* **2011**, *112* (1), 87–93.

(4) Titov, A. N.; Suvorova, O. N.; Ketkov, S. Y.; Titova, S. G.; Merentsov, A. I. Synthesis and Investigation of Titanium Diselenide Intercalated with Ferrocene and Cobaltocene. *Phys. Solid State* **2006**, *48* (8), 1466–1471.

(5) Tazuke, Y.; Takeyama, T. Magnetic Properties of 3d Transition Element Intercalated Compounds M x TiSe 2. *J. Phys. Soc. Japan* **1997**, *66* (3), 827–830.

(6) Shkvarina, E. G.; Titova, S. G.; Titov, A. N.; Shkvarin, A. S. The Mechanism of the Formation of One-Dimensional Chains of the Iron and Vanadium Atoms in the TiSe2 Interlayer Space. *J. Alloys Compd.* **2017**, *717*.

(7) Levy, F.; Froidevaux, Y. Structural and Electrical Properties of Layered Transition Metal Selenides VxTi1-XSe2 and TaxTi1-XSe2. *J. Phys. C Solid State Phys.* **1979**, *12* (3), 473.

(8) Di Salvo, F. J.; Waszczak, J. V. Transport Properties and the Phase Transition in Ti1−xMxSe2 (M=Ta or V). *Phys. Rev. B* **1978**, *17* (10), 3801–3807.

(9) Shkvarin, A. S.; Merentsov, A. I.; Yarmoshenko, Y. M.; Shkvarina, E. G.; Zhukov, Y. M.; Titov, A. A.; Titov, A. N. Electronic Structure of V x Ti 1−x Se 2 in Wide Concentration Region ($0.06 \leq x \leq 0.9$). *J. Chem. Phys.* **2017**, *146* (16), 164703.

(10) Di Salvo, F. J.; Moncton, D. E.; Waszczak, J. V. Electronic Properties and Superlattice Formation in the Semimetal TiSe2. *Phys. Rev. B* **1976**, *14* (10), 4321–4328.

(11) Cercellier, H.; Monney, C.; Clerc, F.; Battaglia, C.; Despont, L.; Garnier, M. G.; Beck, H.; Aebi, P.; Patthey, L.; Berger, H.; et al. Evidence for an Excitonic Insulator Phase in 1T−TiSe2. *Phys. Rev. Lett.* **2007**, *99* (14), 146403.

(12) Rossnagel, K.; Kipp, L.; Skibowski, M. Charge-Density-Wave Phase Transition in 1T−TiSe2: Excitonic Insulator versus Band-Type Jahn-Teller Mechanism. *Phys. Rev. B* **2002**, *65* (23), 235101.

(13) Joe, Y. I.; Chen, X. M.; Ghaemi, P.; Finkelstein, K. D.; de la Peña, G. A.; Gan, Y.; Lee, J. C. T.; Yuan, S.; Geck, J.; MacDougall, G. J.; et al. Emergence of Charge Density Wave Domain Walls above the Superconducting Dome in 1T-TiSe 2. *Nat. Phys.* **2014**, *10* (6), 421–425.

(14) Hellgren, M.; Baima, J.; Bianco, R.; Calandra, M.; Mauri, F.; Wirtz, L. Critical Role of the Exchange Interaction for the Electronic Structure and Charge-Density-Wave Formation in TiSe2. *Phys. Rev. Lett.* **2017**, *119* (17), 176401.

(15) van Bruggen, C. F.; Haas, C. Magnetic Susceptibility and Electrical Properties of VSe2 Single Crystals. *Solid State Commun.* **1976**, *20* (3), 251–254.

(16) Whittingham, M. S. The Electrochemical Characteristics of VSe2 in Lithium Cells. *Mater. Res. Bull.* **1978**, *13* (9), 959–965.

(17) Hughes, H. P.; Webb, C.; Williams, P. M. Angle Resolved Photoemission from VSe 2. *J. Phys. C Solid State Phys.* **1980**, *13* (6), 1125–1138.

(18) Li, F.; Tu, K.; Chen, Z. Versatile Electronic Properties of VSe 2 Bulk, Few-Layers, Monolayer, Nanoribbons, and Nanotubes: A Computational Exploration. *J. Phys. Chem. C* **2014**, *118* (36), 21264–21274.

(19) Pásztor, Á.; Scarfato, A.; Barreteau, C.; Giannini, E.; Renner, C. Dimensional Crossover of the Charge Density Wave Transition in Thin Exfoliated VSe 2. *2D Mater.* **2017**, *4* (4), 041005.

(20) Liu, J.; Hou, W.-J.; Cheng, C.; Fu, H.-X.; Sun, J.-T.; Meng, S. Intrinsic Valley Polarization of Magnetic VSe 2 Monolayers. *J. Phys. Condens. Matter* **2017**, *29* (25), 255501.

(21) Rimmington, H. P. B.; Balchin, A. A.; Tanner, B. K. Nearly Perfect Single Crystals of Layer Compounds Grown by Iodine Vapour-Transport Techniques. *J. Cryst. Growth* **1972**, *15* (1), 51–56.

(22) Brezhestovskii, M. S.; Suslov, E. A.; Bushkova, O. V.; Merentsov, A. I.; Titov, A. N. Influence of Heterovalent Substitution in the Titanium Sublattice on the Electrochemical Intercalation of Lithium in M y Ti1–y Se2 (M = Cr, V)). *Phys. Solid State* **2015**, *57* (10), 2078–2086.

(23) Balagurov, A. M. Scientific Reviews: High-Resolution Fourier Diffraction at the IBR-2 Reactor. *Neutron News* **2005**, *16* (3), 8–12.

(24) Rodríguez-Carvajal, J. Recent Advances in Magnetic Structure Determination by Neutron Powder Diffraction. *Phys. B Condens. Matter* **1993**, *192* (1–2), 55–69.

(25) Prince, E.; Wilson, A. J. C. International Tables for Crystallography. **2004**.

(26) Baranov, N. V; Ibrahim, P. N. G.; Selezneva, N. V; Gubkin, A. F.; Volegov, A. S.; Shishkin, D. A.; Keller, L.; Sheptyakov, D.; Sherstobitova, E. A. Layer-Preferential Substitutions and Magnetic Properties of Pyrrhotite-Type Fe 7− y M y X 8 Chalcogenides (X = S, Se; M = Ti, Co). *J. Phys. Condens. Matter* **2015**, *27* (28), 286003.

(27) Zangrando, M.; Finazzi, M.; Paolucci, G.; Comelli, G.; Diviacco, B.; Walker, R. P.; Cocco, D.; Parmigiani, F. BACH, the Beamline for Advanced Dichroic and Scattering Experiments at ELETTRA. *Rev. Sci. Instrum.* **2001**, *72* (2), 1313.

(28) Stavitski, E.; de Groot, F. M. F. The CTM4XAS Program for EELS and XAS Spectral Shape Analysis of Transition Metal L Edges. *Micron* **2010**, *41* (7), 687–694.

(29) Shkvarin, A. S.; Yarmoshenko, Y. M.; Merentsov, A. I.; Píš, I.; Bondino, F.; Shkvarina, E. G.; Titov, A. N. Guest–Host Chemical Bonding and Possibility of Ordering of Intercalated Metals in Transition-Metal Dichalcogenides. *Inorg. Chem.* **2018**, *57* (9), 5544–5553.

(30) Shkvarin, A. S.; Yarmoshenko, Y. M.; Merentsov, A. I.; Zhukov, Y. M.; Titov, A. A.; Shkvarina, E. G.; Titov, A. N. Electronic Structure of Ni x TiSe 2 (0.05 ≤ x ≤ 0.46) Compounds with Ordered and Disordered Ni. *Phys. Chem. Chem. Phys.* **2017**, *19* (6), 4500–4506.

(31) Yablonskikh, M. V.; Shkvarin, A. S.; Yarmoshenko, Y. M.; Skorikov, N. A.; Titov, A. N. Resonant Photoemission at the L 3 Absorption Edge of Mn and Ti and the Electronic Structure of 1T-Mn 0.2TiSe 2. *J. Phys. Condens. Matter* **2012**, *24* (4).

(32) Shkvarin, A. S.; Yarmoshenko, Y. M.; Merentsov, A. I.; Shkvarina, E. G.; Suslov, E. A.; Brezhestovsky, M. S.; Bushkova, O. V.; Titov, A. N. Chemical Bond in FexTiSe2 Intercalation Compounds: Dramatic Influence of Fe Concentration. *RSC Adv.* **2016**, *6* (108), 106527–106539.

(33) Shkvarin, A. S.; Yarmoshenko, Y. M.; Skorikov, N. A.; Yablonskikh, M. V.; Merentsov, A. I.; Shkvarina, E. G.; Titov, A. N. Electronic Structure of Titanium Dichalcogenides TiX 2 (X = S, Se, Te). *J. Exp. Theor. Phys.* **2012**, *114* (1), 150–156.

(34) Bachrach, R. Z. *Synchrotron Radiation Research: Advances in Surface and Interface Science Techniques*; Springer Science & Business Media, 2012; Vol. 1.

(35) Kay, A.; Arenholz, E.; Mun, S.; Abajo, F. J. G. de; Fadley, C. S.; Denecke, R.; Hussain, Z.; Hove, M. A. Van. Multi-Atom Resonant Photoemission: A Method for Determining Near-Neighbor Atomic Identities and Bonding. *Science (80-.).* **1998**, *281* (5377), 679–683.

(36) Rubensson, J.-E.; Lüning, J.; Eisebitt, S.; Eberhardt, W. It's Always a One-Step Process. *Appl. Phys. A Mater. Sci. Process.* **1997**, *65* (2), 91–96.

(37) Mårtensson, N.; Weinelt, M.; Karis, O.; Magnuson, M.; Wassdahl, N.; Nilsson, A.; Stöhr, J.;

Samant, M. Coherent and Incoherent Processes in Resonant Photoemission. *Appl. Phys. A Mater. Sci. Process.* **1997**, *65* (2), 159–167.

(38) Hüfner, S.; Yang, S.-H.; Mun, B. S.; Fadley, C. S.; Schäfer, J.; Rotenberg, E.; Kevan, S. D. Observation of the Two-Hole Satellite in Cr and Fe Metal by Resonant Photoemission at the 2 p Absorption Energy. *Phys. Rev. B* **2000**, *61* (19), 12582–12585.

(39) Yarmoshenko, Y. M.; Shkvarin, A. S.; Yablonskikh, M. V.; Merentsov, A. I.; Titov, A. N. Localization of Charge Carriers in Layered Crystals Me x TiSe 2 (Me = Cr, Mn, Cu) Studied by the Resonant Photoemission. *J. Appl. Phys.* **2013**, *114* (13), 133704.

(40) de Groot, F. M. F.; Fuggle, J. C.; Thole, B. T.; Sawatzky, G. A. L 2,3 x-Ray-Absorption Edges of D0 Compounds: K+, Ca2+, Sc3+, and Ti4+ in Oh (Octahedral) Symmetry. *Phys. Rev. B* **1990**, *41* (2), 928–937.

(41) Friend, R. H.; Yoffe, A. D. Electronic Properties of Intercalation Complexes of the Transition Metal Dichalcogenides. *Adv. Phys.* **1987**, *36* (1), 1–94.

(42) Shkvarin, A. S.; Yarmoshenko, Y. M.; Skorikov, N. A.; Yablonskikh, M. V.; Merentsov, A. I.; Shkvarina, E. G.; Titov, A. N. Resonance Photoelectron Spectroscopy of TiX2 (X = S, Se, Te) Titanium Dichalcogenides. *J. Exp. Theor. Phys.* **2012**, *115* (5), 798–804.

(43) Piper, L. F. J.; DeMasi, A.; Cho, S. W.; Preston, A. R. H.; Laverock, J.; Smith, K. E.; West, K. G.; Lu, J. W.; Wolf, S. A. Soft X-Ray Spectroscopic Study of the Ferromagnetic Insulator V0.82Cr0.18O. *Phys. Rev. B* **2010**, *82* (23), 235103.

For Table of Contents Only

During intercalation V_xTiSe_2 the charge transfer to the $Ti3d_z^2$ / $V3d_z^2$ band of hybrid states occurs, whereas in the case of substitution $V_xTi_{1-x}Se_2$, the charge remains localized in the vanadium sublattice. The valence band spectra at the Ti 2p-3d and V2p-3d resonant excitation mode show the spatial distribution of the 3d electrons of Ti and V.

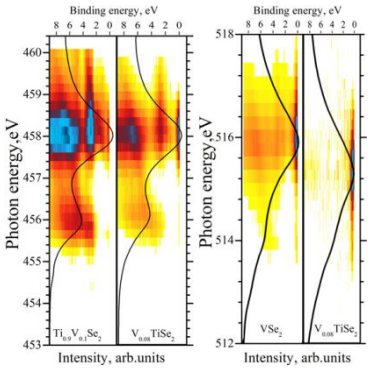

Supporting Information

Electronic structure of the vanadium intercalated and substitutionally doped transition metal dichalcogenides $Ti_xV_ySe_2$

Alexey S. Shkvarin[1,*], Yury M. Yarmoshenko[1], Alexander I. Merentsov[1], Elena G. Shkvarina[1], Andrei F. Gubkin[1], Igor Píš[2,3], Silvia Nappini[3], Federica Bondino[3], Ivan A. Bobrikov[4], Alexander N. Titov[1]

[1]M.N. Miheev Institute of Metal Physics of Ural Branch of Russian Academy of Sciences, 620990 Ekaterinburg, Russia

[2]Elettra-Sincrotrone Trieste S.C.p.A, S.S. 14 – km 163.5, 34149 Basovizza, Trieste, Italy

[3]IOM-CNR, Laboratorio TASC, S.S. 14 – km 163.5, 34149 Basovizza, Trieste, Italy

[4]Joint Institute for Nuclear Research, ul. Joliot-Curie 6, 141980 Dubna, Moscow oblast, Russia

*shkvarin@imp.uran.ru

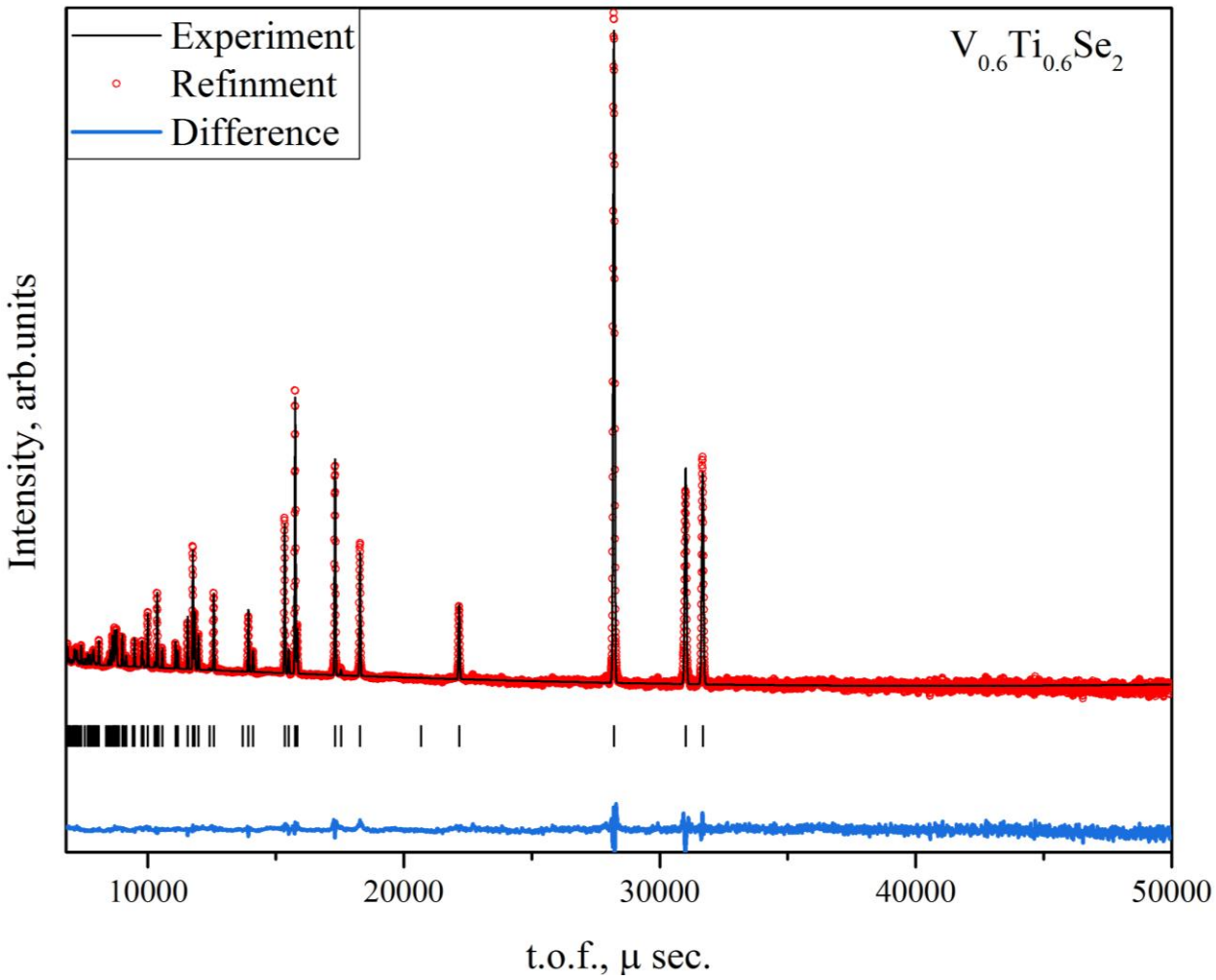

Figure S1. Neutron diffraction patterns for $V_{0.6}Ti_{0.6}Se_2$. Bold lines are experimental data; red points are Rietveld refinement with FullProf. Below the patterns, vertical lines point to the positions of nuclear reflections, blue solid line at the bottom shows the difference between the experimental and calculated patterns.